Supporting Information

Electric Field Reversal of Na_2SO_4, $(NH_4)_2SO_4$, and Na_2CO_3 relative to $CaCl_2$ and NaCl at the Air/Aqueous Interface revealed by Heterodyne Detected Phase-Sensitive Sum Frequency

Wei Hua, Aaron M. Jubb, and Heather C. Allen*

Department of Chemistry, The Ohio State University, 100 West 18th Ave, Columbus, OH, 43210

allen@chemistry.ohio-state.edu

Re $\chi^{(2)}$ spectra

The Re $\chi^{(2)}$ spectra of water molecules at vapor/aqueous solution interfaces are shown in Figure S1. The result of spectral convolution of the Im $\chi^{(2)}$ component with the Re $\chi^{(2)}$ component accounts for the changes of spectral line shape relative to the neat water spectrum observed with conventional VSFG (Fig. 1a). In the case of the calcium chloride salt solution VSFG spectrum (Fig. 1a), this convolution explains the enhancement of the 3300 cm^{-1} feature, whereas for the other salt solutions convolution with the Re $\chi^{(2)}$ component does not produce significant spectral change.

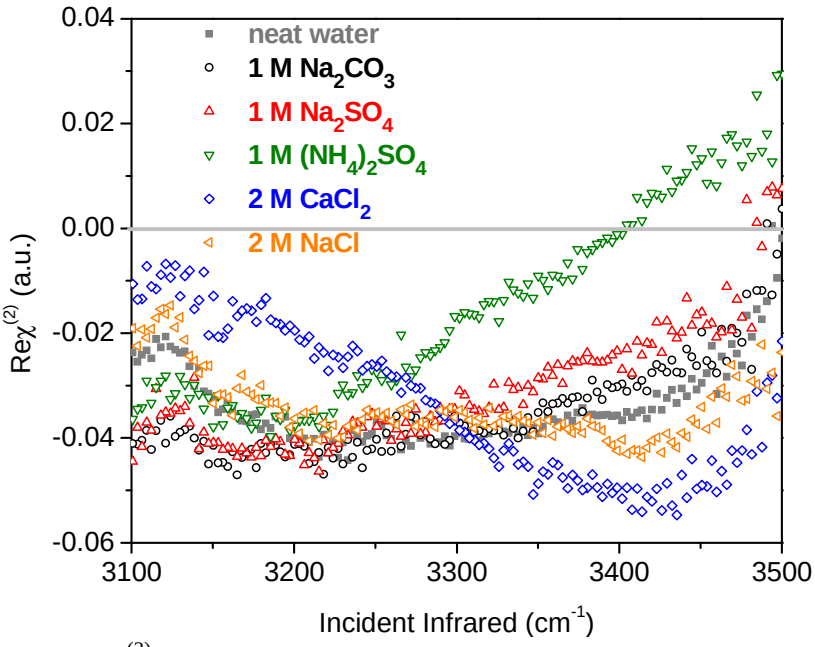

Figure S1. PS-SFG Re $\chi^{(2)}$ spectra of water molecules at vapor/aqueous solution interfaces of neat water, 1.8 M $CaCl_2$, 1.8 M NaCl, 1.1 M Na_2CO_3, 1.1 M Na_2SO_4, and 1.1 M $(NH_4)_2SO_4$ salt solutions.

Experimental Methods and Data Processing Procedures

A titanium:sapphire oscillator (792 nm) – double regenerative amplifier system (1 kHz) (Spectra-Physics) was used for the visible and infrared light generation. The amplifiers generate a visible beam of 2 ps pulses at 792 nm (17 cm^{-1} bandwidth, > 500 mW), while ~ 85 fs pulses at 792 nm (22 nm bandwidth, > 1 W) are used to generate a tunable broadband infrared beam in an optical parametric amplifier (Light Conversion, TOPAS). This is followed by a nonlinear difference-frequency generation system (Light Conversion, NDFG connected to the TOPAS). The full spectral bandwidth of the generated broadband infrared beam is ~500 cm^{-1} in the region under investigation and the average power of the visible beam and the infrared beam were 300 μJ and 10 μJ, respectively. The visible beam, s-polarized and 792 nm, and the infrared beam , p-polarized, were spatially and temporally overlapped on the sample stage (for samples and z-cut quartz) with incident angles of ~50˚ and ~60˚, respectively, to generate the sum frequency beam, which was s-polarized.

The PS-SFG sample and detection setup used here is similar to the system reported by Tahara and co-workers,[1] which is based on heterodyne detection of broad band intensities and Fourier transform analysis. The important part of the optical configuration in our SFG system was redesigned for the PS-SFG application as is illustrated in Figure S2.[2,3]

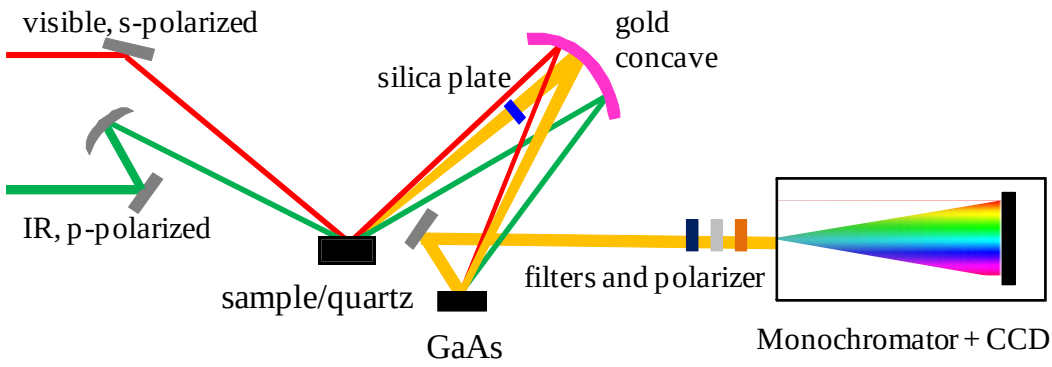

Figure S2. Schematic of the heterodyne-detected PS-SFG optical configuration. Filters and polarizer denote two short-pass filters, a notch filter, and a Glan-Thompson polarizer respectively from left to right.

After reflection from the sample/reference, the incident visible, infrared, and generated sum frequency (s-polarized) beams were refocused by a gold concave mirror (f = 100 mm) onto a GaAs (Lambda Precision Optics) surface to generate another sum frequency beam (local oscillator, LO). The two sum frequency beams from different stages generated an interference fringe in the frequency domain by passing the sum frequency beam generated from the sample (or quartz reference) through a 1 mm thick silica plate positioned before the gold concave mirror, resulting in a time delay of ~2.6 ps. The interferogram was stretched in a monochromator (Acton Research, SpectraPro SP-500 monochromator with a 1200 g/mm grating blazed at 750 nm) and detected by a liquid-nitrogen cooled charge-coupled device (CCD) (Roper Scientific, 1340 × 400 pixel array, Spec-10:400B: LN400EB back illuminated CCD). Special attention was given to the shape of image on the CCD array. If the image was slightly tilted, data points were consistently shifted relative to the central pixel line on the image to avoid integrated signal attenuation. The height of the sample surface was checked by the image on the CCD. Retaining

the same height is critical for accurate phase determination. During the experiments, the height of the reference surface (quartz) and the sample surface were identical, within our measurement ability. Neat water was used as a reference for the pixel height. Height accuracy was better than 3 μm, where each CCD pixel is 20 x 20 μm.

The total detected intensity can be described as:[1]

$$I_{HD-SFG} \propto \left|E_{tot}\right|^2 = \left|E_{sample} + E_{LO}\right|^2$$

$$= \left|E_{sample}\right|^2 + \left|E_{LO}\right|^2 + E_{sample}{E_{LO}}^* \exp(i\omega\Delta t) + {E_{sample}}^* E_{LO} \exp(-i\omega\Delta t)$$

E_{sample} denotes the sum frequency beam from samples or quartz and E_{LO} denotes the sum frequency beam from GaAs. Δt is the ~2.6 ps time difference between two sum frequency beams.

The raw interferograms (Figure S3) were inverse Fourier transformed to the time domain using OriginPro software (version 7.5). The $|E_{sample}|^2$ and $|E_{LO}|^2$ signals at t = 0 in time domain were filtered out and only the cross terms were kept and followed by Fourier transform back to the frequency domain. The resulting frequency spectra contain phase information (φ) of the complex $E_{sample}{E_{LO}}^* exp(i\omega\Delta t)$ (Figure S3). The quartz spectrum was used as a reference, because quartz did not have any apparent resonance in this infrared region, and the phase of quartz was regarded as a constant. Therefore, the real and imaginary $\chi^{(2)}$ spectra can be obtained by dividing the sample interferogram by the quartz reference spectrum through which the contribution from E_{LO} is completely removed.

The final spectra were normalized to the reflectivities of the incident visible and IR beams on quartz and on the samples. The expression of the Im $\chi^{(2)}$ spectrum is as follows:

$$\mathrm{Im}\,\chi^{(2)} \propto \frac{r_{vis,quartz} r_{IR,quartz} \left|E_{sample} E_{LO}\right|}{r_{vis,sample} r_{IR,sample} \left|E_{quartz} E_{LO}\right|} \sin(\varphi_{sample} - \varphi_{quartz})$$

r is the reflectivity of the incident visible or IR beams on quartz or the sample. The phases of the quartz and sample (φ) were obtained directly from the Fourier transformation. Final spectra were averaged over the two consecutive runs with 5 min integration times for each sample. The measured reproducibility of the intensity when the sample was changed was within 5%.

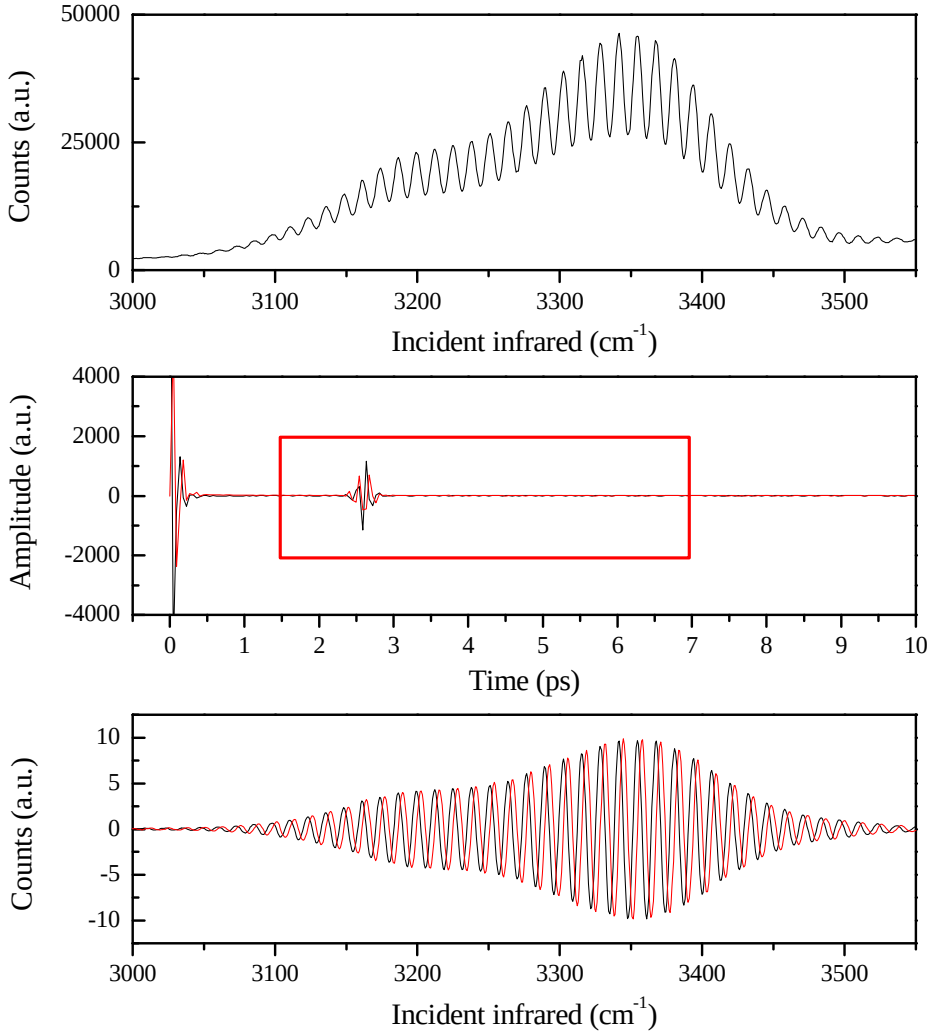

Figure S3. Upper panel: Raw interferogram of z-cut quartz with GaAs. Middle panel: Time domain real (black) and imaginary (red) signals. The cross term at ~ 2.6 ps is extracted to yield the heterodyne frequency spectra. Lower panel: Real (black) and imaginary (red) parts of heterodyne frequency spectra of z-cut quartz with GaAs. Phase information (φ) is therefore obtained.

The heterodyne-detected PS-SFG spectra are shown in the main manuscript and here from 3000 to 3500 cm^{-1}. Our current IR profile has intensity that is lower near 3100 cm^{-1} as compared to 3400 cm^{-1} (Figure S3, upper panel), which can slightly distort the normalized intensity near 3100 cm^{-1}. Work is under way in our laboratory to further expand our available

PS-SFG bandwidth.

To discuss the delicate spectral changes in the air/aqueous interface the phase stability and accuracy need to be carried out with extreme care. As mentioned above, when doing data processing, the Im $\chi^{(2)}$ of the neat water is calculated from normalizing the phase of neat water (φ_{sample}) by the phase of quartz reference (φ_{quartz}). However, during the experimental operation, the way the quartz reference is mounted on the sample stage was imperfect, so the phase (angle) of z-cut quartz might vary on different days. This may result in an uncertainty with assigning the absolute phase of our quartz reference; work is underway in our laboratory to improve this. Therefore, a phase drift of the quartz reference could be observed occasionally and hence a phase correction procedure was applied with respect to our previously obtained averaged quartz phase data to eliminate (or compensate) for this uncertainty. Our spectral resolution (and reproducibility) are less than optimal and our water Im $\chi^{(2)}$ spectrum, hence, has a 20˚±5˚ phase resolution (uncertainty). This is the main reason for the shift of the crossing point in the published Im $\chi^{(2)}$ spectrum for neat water[2,3] and this manuscript.

Critical here is that all Im $\chi^{(2)}$ spectra of salt solutions are compared to the neat water Im $\chi^{(2)}$ spectrum. Thus our interpretation is mainly based on the *relative* difference from neat water to that of the salt solution systems. During daily operation, the quartz reference was never moved when measuring the spectra for neat water and all the salt solution samples, and the water sample was re-measured around every three hours to ensure the stability and reproducibility of the phase of the water Im $\chi^{(2)}$ spectrum obtained in the same day. This ensured reliable phase reproducibility between measured neat water and salt solutions Im $\chi^{(2)}$ spectra. Here, replicate Im $\chi^{(2)}$ spectra of neat water, 1.1 M Na_2CO_3, 1.8 M $CaCl_2$ and 1.8 M NaCl salt solutions measured on different days are shown in Figure S4. Although fine spectral line shape changes are observed, the general shape of Im $\chi^{(2)}$ spectra on different days for the same sample agree within experimental error. The relative difference observed in the Im $\chi^{(2)}$ spectra were reproduced on different days.

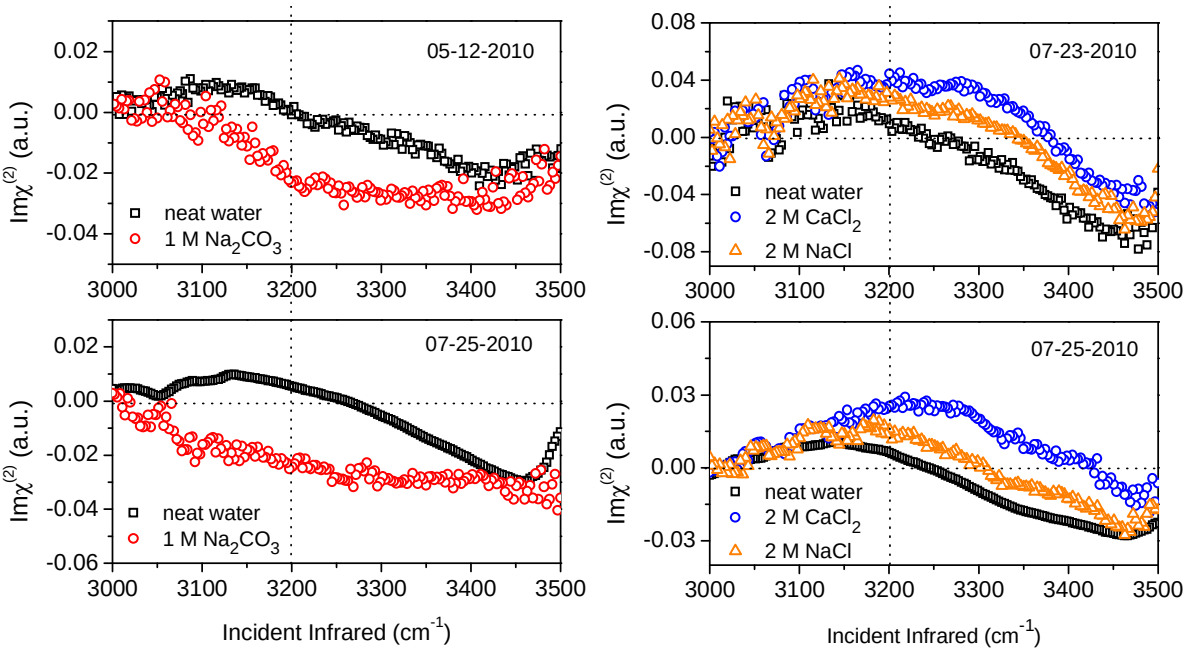

Figure S4: Reproducibility testing: Im $\chi^{(2)}$ spectra of neat water, 1.1 M Na_2CO_3, 1.8 M $CaCl_2$ and NaCl salt solutions measured on different days.

References

(1) Nihonyanagi, S.; Yamaguchi, S.; Tahara, T. Direct Evidence for Orientational Flip-Flop of Water Molecules at Charged Interfaces: A Heterodyne-Detected Vibrational Sum Frequency Generation Study. *J. Chem. Phys.* **2009**, *130*, 204704-204704.

(2) Chen, X. K.; Hua, W.; Huang, Z. S.; Allen, H. C. Interfacial Water Structure Associated with Phospholipid Membranes Studied by Phase-Sensitive Vibrational Sum Frequency Generation Spectroscopy. *J. Am. Chem. Soc.* **2010**, *132*, 11336-11336.

(3) Hua, W.; Chen, X. K.; Allen, H. C. Phase-Sensitive Sum Frequency Revealing Accommodation of Bicarbonate Ions, and Charge Separation of Sodium and Carbonate Ions within the Air/Water Interface. *J. Phys. Chem. A* **2011**, *115*, 6233-6233.